https://dx.doi.org/10.21577/0103-5053.20200073

J. Braz. Chem. Soc., Vol. 31, No. 9, 1852-1858, 2020
Printed in Brazil - ©2020 Sociedade Brasileira de Química

Article

Crystallographic Changes Accompanying the Verwey Transition in a Magnetite from Steatite

Fernando D. da Silva,[a,b] *Sandra L. Nogueira,*[b] *José D. Fabris,*[a] *Antônio T. Goulart*[a] *and Paulo R. C. Couceiro*[c]

[a]*Departamento de Química, Universidade Federal de Minas Gerais, Campus Pampulha, 31270-901 Belo Horizonte-MG, Brazil*

[b]*Centro Universitário de Patos de Minas, UNIPAM, 31708-054 Patos de Minas-MG, Brazil*

[c]*Departamento de Química, Universidade Federal do Amazonas, 69077-000 Manaus-AM, Brazil*

The crystallographic structural analysis of the magnetite of a steatite rock at 298 K, (saturation magnetization, σ = 95.0 J T^{-1} kg^{-1}) showed two cubic networks and, below Verwey temperature (T_V ca.120 K) a monoclinic structure, basing on their cell dimensions and different transitional behaviors when reducing the temperature. A monoclinic structure was identified from their cell dimensions and different transition behaviors when reducing the temperature. The average chemical formula of this almost stoichiometric magnetite was deduced from the chemical analysis, 298 K-Mössbauer and the structural refinement. The Rietveld fitting of the 298 K X-ray pattern is $[Fe^{3+}]\{Fe^{3+}_{0.95}Fe^{2+}_{0.88}Cr^{3+}_{0.04}Al^{3+}_{0.04}Mg^{2+}_{0.05}Ni^{2+}_{0.02}\otimes_{0.02}\}\ O_4$, where [ ] and { } stand for cations in tetrahedral and octahedral coordination symmetries, respectively. The crystallographic structure below T_V in this magnetite was observed from synchrotron X-ray diffraction data (XRD), collected at 15 K. It was identified three structures: two cubic (space group, Fd3m), with significantly different lattice parameters, and one monoclinic (P2/c).

Keywords: magnetite, Rietveld, Verwey transition

Introduction

Magnetite (ideal formula, Fe_3O_4; cubic, space group Fd3m) is a ferrimagnetic iron oxide with an inverted spinel structure.[1,2] In nature, magnetite is often oxidized to hematite (αFe_2O_3, hexagonal, space group $R\bar{3}c$),[3] a thermodynamically more stable ferric oxide, either directly or via an intermediate formation of maghemite (γFe_2O_3 or, in the equivalent chemical structure of a ferric spinel, $Fe^{3+}_{\frac{8}{3}}\otimes_{\frac{1}{3}}O_4$; $\otimes$ = vacancy),[4] which also crystallizes in space group Fd3m. The crystallochemical steps governing the transformation magnetite → maghemite are still a focus of attention and controversy.[5-7] Reported data in the literature suggest that, under comparable natural conditions, the whole mechanism depends upon the nature of the magnetite precursor, including its chemical composition and crystal size.[8]

Magnetite undergoes a first order structural change from cubic to monoclinic at T_v = 120 K, the Verwey temperature, which was first reported about seventy years ago.[9-11] Below T_v, the electrical resistivity of the oxide increases by two orders of magnitude. According to Verwey,[12,13] the high conductivity of magnetite at higher temperatures would be due to the fast electron transfer between Fe^{2+} and Fe^{3+} ions in the octahedral sites. At $T < T_v$, the Fe^{2+} and Fe^{3+} ions tend to be increasingly ordered, towards ceasing the electron transfer process. This transition is very sensitive to particle size, degree of $Fe^{2+} \rightarrow Fe^{3+}$ oxidation and isomorphical replacement of iron by other cations.[14]

A detailed structural analysis of magnetite in natural samples, such as from soil, is a challenging task, particularly due to the complex nature of the material, not rarely presenting a large number of coexisting phases. As a result of this complexity, powder X-ray diffraction (XRD) patterns usually show a great deal of superposed reflections that can be better addressed with the Rietveld method.[15] Other analytical techniques, such as ^{57}Fe Mössbauer spectroscopy, can provide valuable information about the local environment of the iron ions in the crystalline structure as well as information about its chemical state, even in amorphous materials. This work aimed at characterizing,

*e-mail: fernandosilva@unipam.edu.br

mainly by ^{57}Fe Mössbauer spectroscopy and XRD, a magnetite obtained from a steatite rock sample collected in the Quadrilátero Ferrífero area (Minas Gerais state, Brazil), in an attempt to follow its essential crystallographic characteristics, by varying the temperature, above and below T_v.

Experimental

Steatite rock lumps (about 20 to 40 cm-long) were collected at approximately 3 m deep from the soil surface, from a sampling site (geographical coordinates, 20º30'38.6"S 43º50'18.7"W) in the Quadrilátero Ferrífero area, state of Minas Gerais state, Brazil. The magnetic fraction from the rock samples was magnetically separated with a hand magnet, from the ground rock material. These magnetic samples were submitted to a chemical treatment with citrate-bicarbonate-dithionite (CBD), according to the procedure described by Mehra and Jackson,[16] intending to remove mainly free hematite.

The chemical analysis of the magnetic fractions was carried out by dissolving the sample with hydrochloric acid 1:1 (v/v). The solution obtained was then analyzed for Fe by the standard dichromatometric method.[17] Contents of Al, Cr, Mn and Ni in the supernatant solution were read in an inductively-coupled plasma atomic emission spectroscopy (ICPAES) equipment, model Spectroflame, from Analytical Instruments.

Saturation magnetization measurements were made with a portable magnetometer.[18] The scanning electron micrograph of the sample was recovered with a gold-sputtered thin film obtained with a JEOL JSM-840 A equipment.

Mössbauer spectra were obtained at room temperature (ca. 298 K) using a conventional constant acceleration spectrometer. Transmission spectra were obtained with a conventional transmission setup and a radiation source, with a nominal activity of ca. 50 mCi ^{57}Co, in a Rh matrix. Spectra were stored in 512 channels memory unit in the multi-scaling mode, with the Doppler velocity ranging about ± 10 mm s^{-1}, calibrated with a metallic iron (αFe) foil absorber. Absorbers, with a uniform thickness corresponding to ca. 10 mg Fe cm^{-2}, were prepared by mixing the magnetic powder samples with sucrose. The obtained experimental data were fitted to Lorentzian-shape line functions by the least-square fitting statistical procedure, with the NORMOS-90™-computer program.[19]

XRD data were obtained for the magnetic fraction with particles size corresponding to the sieved material retained by a sieve with openings of 20 μm. XRD powder patterns were collected with the sample at 300, 150, 100, 50 and 15 K (± 2 ºC), using an X-ray powder diffractometer, with the synchrotron radiation source of the XPD line of the Brazilian Synchrotron Light Laboratory (LNLS, Campinas, SP, Brazil), set to a wavelength λ = 0.176041 nm, in the step-scanning mode, and counting radiation of 1 s in 0.005º 2θ-increments between 18 and 80º 2θ. Powder silicon was used as an external standard.

The Rietveld structural refinement from XRD data was performed with the FULLPROF program (June 2007 version).[20]

Results and Discussion

Table 1 shows the chemical composition, expressed in mass% of the corresponding cation oxides. The sample was found to contain essentially iron, corresponding to 97.15 mass% Fe_2O_3, along with minor amounts of Al, Cr, Mg and Ni; Si was found to be below the limit of detection of the method.

The measured value of saturation magnetization for the magnetic extract from the rock sample was $\sigma = 95.0$ J T^{-1} kg^{-1}, which is only slightly below the characteristic value for a pure magnetite,[21] σ ca. 100 J T^{-1} kg^{-1}, which suggests a sample in excellent condition (Figure 1).

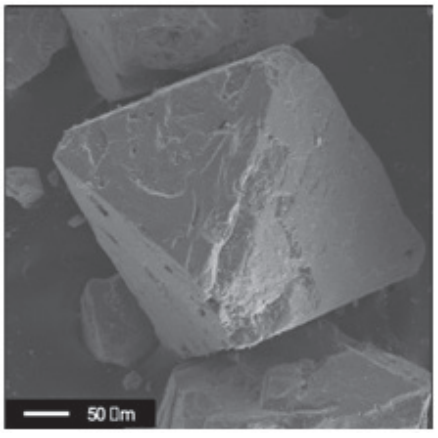

Figure 1. Image of scanning electronic microscopy of the sample, in detail an octahedral crystal.

Table 1. Chemical composition and magnetization of saturation (σ_s) of the magnetic fraction of the rock

Fe_2O_3 / %mass	MnO / %mass	NiO / %mass	Cr_2O_3 / %mass	Al_2O_3 / %mass	σ_s / (J T^{-1} kg^{-1})
97.15(7)	0.04(1)	0.87(8)	2.07(1)	1.01(3)	95.0(1)

σ_s: magnetization of saturation. The values in parentheses are uncertainties of the numerical value, estimated by the standard deviation calculated by the nonlinear minimization algorithm of the quadratic errors, expressed on the last significant figure of the numerical value of the corresponding physical quantity.

The 298 K-Mössbauer spectrum was first decomposed two six-line subspecters, as would be expected for magnetite, but the resonance line for the lower hyperfine field (B_{hf}; site B, octahedral) component appeared somewhat asymmetric. For this reason, this spectral contribution was fitted with a model-independent hyperfine field distribution (Figure 2).

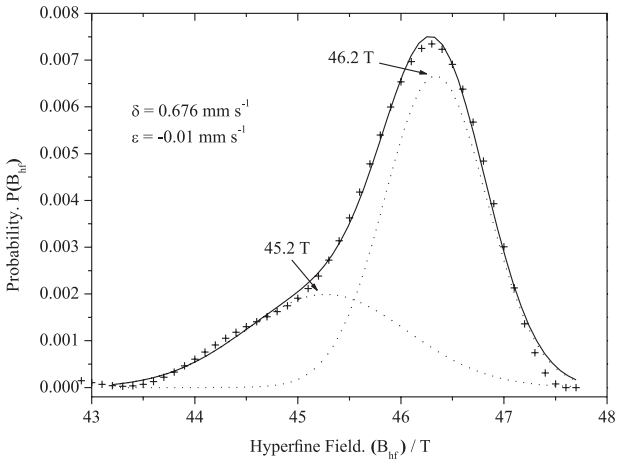

Figure 2. Hyperfine field distribution of probability of the octahedral site (site B) of the magnetite.

This numerical analysis led to two maxima on the probability profile: at B_{hf} = 45.2 and 46.2 T. Following this result, the whole spectrum was then fitted with three Lorentzian-shaped sextets, two of them assigned to B-sites as shown in Figure 3. Resulting hyperfine parameters are presented in Table 2. These data are in accordance with the reported values[22] for the magnetite B-site. Octahedral Fe^{2+} in magnetite is, in variable rate, expected to be oxidized to Fe^{3+}, when exposed to air. In this circumstance the charge re-balance implies the appearance of structural cation vacancies and some diffusion of iron towards the grain surface.[23] The third sub-spectrum was assigned to the A-site with tetrahedral coordination.

Based on the Mössbauer spectroscopy, we conclude that the existence of two hyperfine octahedral sites was the result of a slight crystallographic distortion of one of them, which leads to a small, but still significant, change in the value of the quadrupole displacement, ε = –0.04(1) (Table 2), in relation to the characteristic magnetite (ε = +0.01(1)). This hypothesis is verified in more detail in the XRD data.

The 298 K-XRD pattern (Figure 4) shows well defined reflections, with line-width at half height, 0.0832° 2θ, for

Table 2. Mössbauer parameters at 298 K measured on the magnetic fraction of the rock

Site	Site ^{57}Fe	δ / (mm s^{-1})	ε / (mm s^{-1})	B_{hf} / T	RA / %
Mt_i	octahedral	0.67(2)	–0.04(1)	45.2(1)	29.3(2)
Mt_d	octahedral	0.66(1)	0.01(1)	46.5(2)	35.1(1)
Mt	tetrahedral	0.27(3)	–0.03(1)	49.5(1)	35.6(1)

Mt_i: ideal magnetite; Mt_d: distorted magnetite; Mt: magnetite; δ: isomer shift relative to αFe; ε: quadrupole displacement; B_{hf}: hyperfine field; RA: relative area. The values in parentheses are uncertainties of the numerical value, estimated by the standard deviation calculated by the nonlinear minimization algorithm of the quadratic errors, expressed on the last significant figure of the numerical value of the corresponding physical quantity.

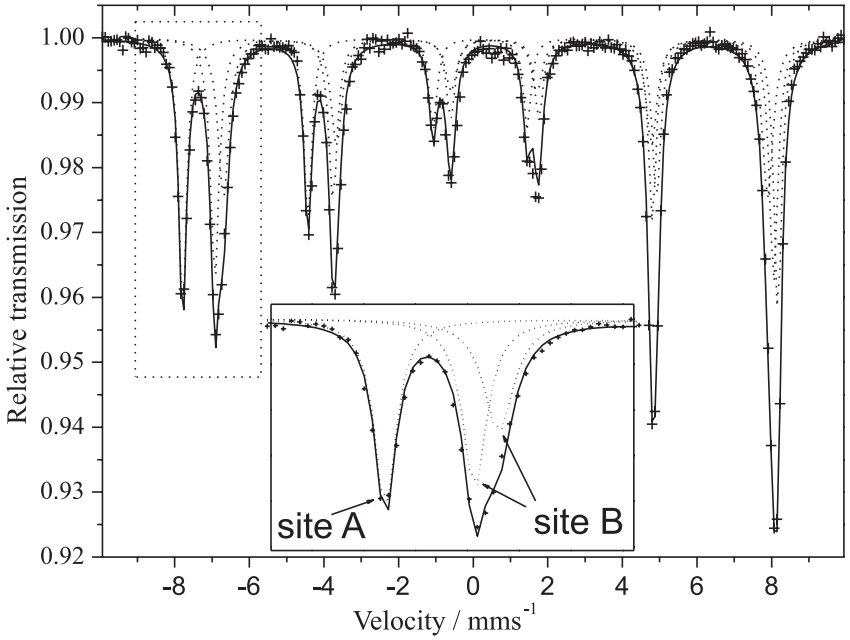

Figure 3. Room temperature-Mössbauer spectrum for the magnetic sample separated from the steatite rock. Inset: details of the resonance line 1 for site A and for the two spectral contributions from the numerically decomposed resonance line due to site B.

the more intense (311) reflection, which are characteristic for the cubic system Fd3m, corresponding to a determined unit cell dimension of a = 0.83959(2) nm. This cell parameter is well comparable with the reported value for magnetite (JCPDS[24] card No. 07-0322, a = 0.83967(3) nm).

To check the consistence of a single-phase or bi-phases pattern, the reflection for the (311) plane was decomposed into two single modified pseudo-Voigt functions. Results presented in Figure 4 really indicate the co-existence of two cubic structures, one of them only very subtly distorted from the ideal crystalline cell of magnetite. This model is consistent with the Mössbauer results and supports the hypothesis that the two hyperfine fields arise from a partial structural distortion of the whole crystallographic framework.

The structural Rietveld refinement[25] of XRD data for the sample at 298 K was performed by taking into account two crystallographic dimensions for the cubic cells. It was used parameters of the width at half the maximum (FWHM)[26] and atomic occupations, including isomorphic substitution of iron. Best results were obtained with the function pseudo-Voigt modified by Thompson-Cox-Hastings.[27]

Figure 5 shows the fitted intensities, corresponding to chi-squared test (χ^2) = 2.18. Resulting values of R_B and R_f factors, lattice parameters and χ^2 are presented in Table 3. Fitted dimensions for these two cubic structures are slightly different from the reported values,[13] certainly due to isomorphic replacements of iron by other cations with different ionic radius, in the magnetite crystalline lattice.

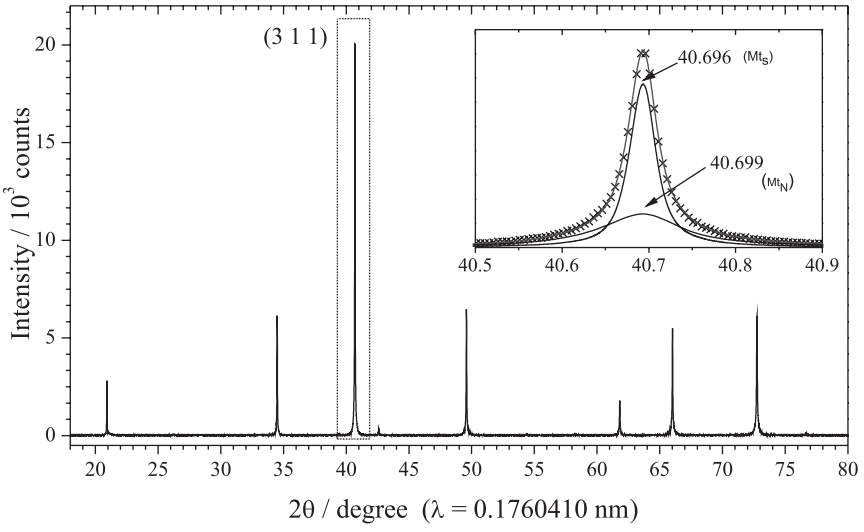

Figure 4. X-ray powder diffraction patterns at 298 K of the magnetic fraction. Deconvolution of the reflection (311) in detail.

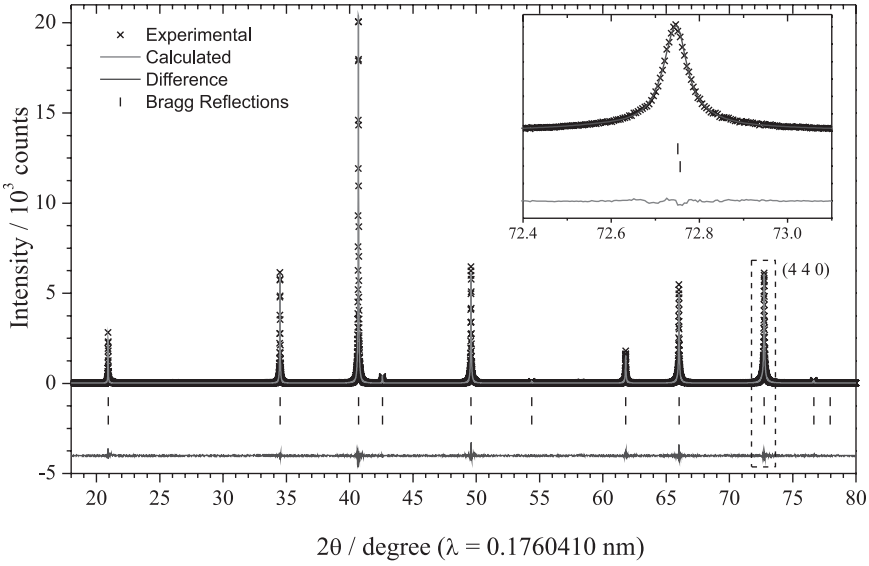

Figure 5. Refinement Rietveld of magnetic fraction powder for data collected at 298 K. Observed (x), calculated (line), and difference (bottom line). The bars indicate the allowed Bragg reflections.

Table 3. Data of the Rietveld refinement at 15 K measured on magnetic fraction of the rock

Phase	Spatial group	Parameter	Temperature / K	
			ca. 298	15
Mt_d	cubic (Fd3m)	*a* / nm	8.3951(3)	0.83873(1)
		proportion in mol / %	47.3	61.5
		R_b	2.31	0.79
		R_f	1.83	0.73
Mt_i	cubic (Fd3m)	*a* / nm	8.3959(1)	0.83863(1)
		proportion in mol / %	52.7	19.4
		R_b	3.27	7.15
		R_f	2.42	3.48
Mt_m	monoclinic (P2/c)	*a* / nm	–	0.59474(2)
		b / nm	–	0.59226(1)
		c / nm	–	1.6782(1)
		proportion in mol / %	–	19.1
		R_b	–	2.99
		R_f	–	5.77
		χ^2	2.18	2.47

Mt_d: distorted magnetite; Mt_i: ideal magnetite; Mt_m: monoclinic magnetite; *a*, *b* and *c*: lattice parameters; R_b: Bragg factor, R_f: structural factor; χ^2: chi-squared test. The values in parentheses are uncertainties of the numerical value, estimated by the standard deviation calculated by the nonlinear minimization algorithm of the quadratic errors, expressed on the last significant figure of the numerical value of the corresponding physical quantity.

The proportions for each of these two cubic phases are Mt_i = 52.7 mol% (ideal cubic) and Mt_d = 47.3 mol% (slightly distorted the cell parameter). These same proportions can be deduced from Mössbauer data (Table 2), meaning that the two groups of hyperfine parameters found for octahedral sites directly reflects on the crystallographic structure of this magnetite.

The estimated chemical formula for Mt_i, also on basing chemical analysis and ionic distribution from the structural refinement, where all isomorphic cations were assumed to occupy octahedral sites, is:[28]

$$[Fe^{3+}]\{Fe^{3+}_{0.95}Fe^{2+}_{0.88}Cr^{3+}_{0.04}Al^{3+}_{0.04}Mg^{2+}_{0.05}Ni^{2+}_{0.02}\otimes_{0.02}\}\,O_4\ (M = 227.73\ g\ mol^{-1}) \quad (1)$$

Chemical elements other than iron were allocated as isomorphic substituents at the octahedral site of the magnetite with cell parameters distorted from the pattern. This change in parameters is characteristic of this type of substitution.

The FWHM of representative reflections and the average particle size were obtained with the Scherrer formula:[29]

$$D_{hkl} = \frac{k\lambda}{\beta_{hkl}\cos\theta_{hkl}} \quad (2)$$

where k is a proportionality constant that depends on the crystals form (in this work, k = 0.9), β is the width half height of the reflection and θ is the position of the reflection. Found $\overline{D}$-values for Mt_i and Mt_d were 253 and 78 nm, respectively.

Figure 6 shows (440)-reflection profiles at varying temperatures. These findings for Mt_i are similar to those reported by Wright,[30,31] confirming a first order structural transition from cubic (Fd3m) to monoclinic (P2/c), on passing the Verwey temperature.

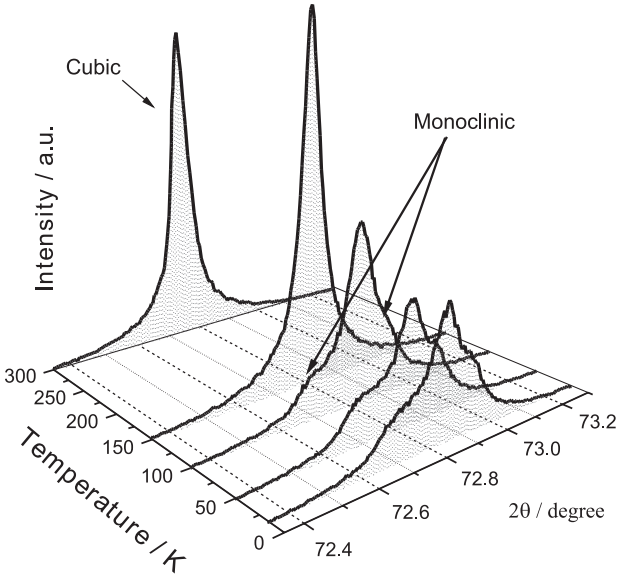

Figure 6. (440) synchrotron X-ray diffraction peak from magnetite below and above the Verwey transition.

These fitted XRD[32,33] patterns (Figure 7) represent a good description of intensities and reflections positions, by taking into account two co-existing cubic (Mt_i and Mt_d) and a monoclinic structure, below T_v. Estimated dimensions for these Mt_i and Mt_d cubic cells, represent differences of about 0.1%.

From 15 K data, proportions including the monoclinic (Mt_m) phase are: Mt_m = 19.1 mol%; Mt_d = 19.4 mol% and Mt_i = 61.5 mol%.

Conclusions

This steatite rock-magnetite (saturation magnetization, $\sigma = 95.0\ J\ T^{-1}\ kg^{-1}$) undergoes the crystallographic Verwey transition of part of its whole crystalline structure, as it could be observed from synchrotron X-ray powder diffraction measurements, collected at 15 K.

The averaged chemical formula for this nearly stoichiometric magnetite, as it could be deduced from

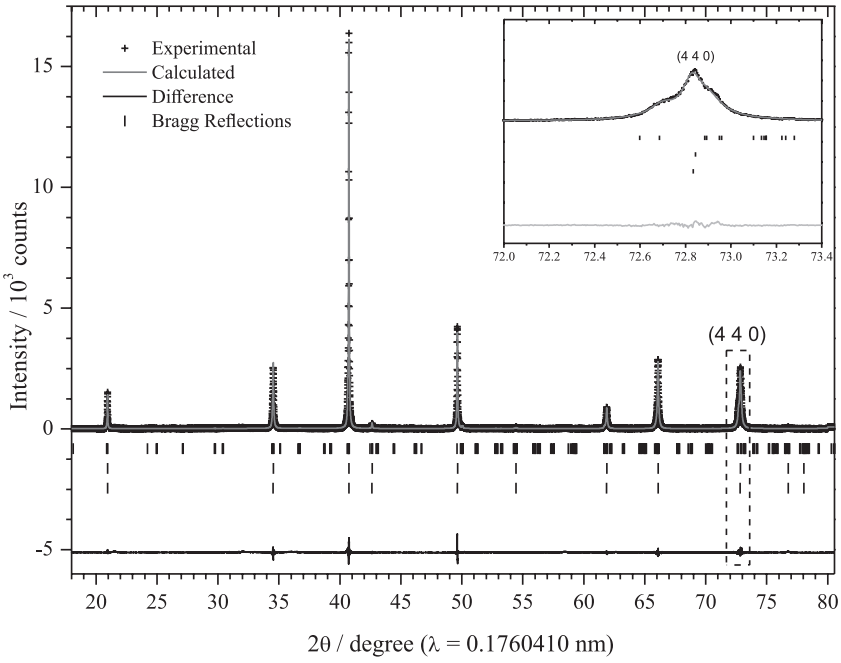

Figure 7. Refinement Rietveld of magnetic fraction powder for data collected at 15 K. Observed (x), calculated (line), and difference (bottom line). The bars indicate the allowed Bragg reflections.

chemical and 298 K-Mössbauer data and from the structural Rietveld fitting of the 298 K X-ray powder pattern is $[Fe^{3+}]\{Fe^{3+}_{0.95}Fe^{2+}_{0.88}Cr^{3+}_{0.04}Al^{3+}_{0.04}Mg^{2+}_{0.05}Ni^{2+}_{0.02}\otimes_{0.02}\}\ O_4$, where [ ] and { } stand for cations in tetrahedral and octahedral coordination symmetries, respectively.

The isomorphic substitution for iron is assumed to respond for the suppressed transition in part of the crystallographic framework: at 15 K, it was identified three co-existing structures: two cubic (space group, Fd3m, accounting for 89.9 mol%), with significantly different lattice dimensions ($a = 0.83873(1)$ and $a = 0.83863(1)$ nm), and one monoclinic (P2/c, 19.1 mol%; $a = 0.5947(3)$ nm, $b = 0.59227(3)$ nm and $c = 1.67823(6)$ nm).

New experimental attempts are being made to follow in more detail the transitional behavior of this system, basing on new synchrotron X-ray diffraction and in-field Mössbauer data, by varying the sample temperature from above T_V down to 15 K.

Acknowledgments

Work supported by CNPq, FAPEMIG (Brazil) and Brazilian National Laboratory of Synchrotron Light (LNLS) in Campinas (SP). Authors also thank Dr F. F. Fereira and Dr E. G. M. da Silva (LNLS) for their technical assistance during XRD data collection, Mr W. T. Soares (Electron Microscopy Laboratory, UFMG), for taking SEM images and EDS data, for Dr A. C. Dorigueto, Mirta Mir (Department of Exact Sciences University of Alfenas) and J. M. Delgado (Department of Chemistry, University of Los Andes) for support with XRD treatment.

References

1. Vandenberghe, R. E.; de Grave, E. In *Mössbauer Spectroscopy Applied to Inorganic Chemistry*, vol. 3, 1st ed.; Long, G. J.; Grandjean, F., eds.; Plenum: New York, 1987, p. 59-182.
2. Santana, G. P.; Fabris, J. D.; Goulart, A. T.; Santana, D. P.; *Rev. Bras. Cienc. Solo* **2001**, *25*, 33.
3. Pinto, M. C. F.; Fabris, J. D.; Goulart, A. T.; Santana, G. P.; *Hyperfine Interact. C* **1998**, *3*, 325.
4. The Verwey Transition, *Philos. Mag. B* **1980**, *42*, 325.
5. Sorescu, L. M.; Diamandescu, R. A.; Tarabasanu-Mihaila, D.; *Mater. Lett.* **2004**, *58*, 885.
6. Goff, R. J.; Wright, J. P.; Attfield, J. P.; Radaelli, P. G.; *J. Phys.: Condens. Matter* **2005**, *17*, 7633.
7. Doriguetto, A. C.; Fernandes, N. G.; Persiano, A. I. C.; Nunes Filho, E.; Greneche, J. M.; Fabris, J. D.; *Phys. Chem. Miner.* **2003**, *30*, 249.
8. Lagoeiro, L. E.; *J. Metamorph. Geol.* **1998**, *16*, 415.
9. Blasco, J.; García, J.; Subías, G.; *Phys. Rev. B* **2011**, *83*, 104105.
10. Verwey, E. J. W.; *Nature* **1939**, *144*, 327.
11. Verwey, E. J. W.; Haayman, P. W.; *Physica* **1941**, *8*, 979.
12. Verwey, E. J. W.; Haaymam, P. W.; Romeijn, F. C. J.; *Chem. Phys.* **1947**, *15*, 181.
13. García, J.; Subías, G.; *J. Phys.: Condens. Matter.* **2004**, *16*, 145.

14. Özdemir, Ö.; Dunlop, D. J.; Moskowitz, B. M.; *Geophys. Res. Lett.* **1993**, *20*, 1671.
15. Rietveld, H. M. J.; *J. Appl. Crystallogr.* **1969**, *2*, 65.
16. Mehra, O. P.; Jackson, M. L. In *Proceedings of Seventh National Conference on Clays and Clay Minerals*; Swineford, A., ed.; Pergamon Press: Washington, 1960, p. 317.
17. Jeffery, P. G.; Hutchison, D.; *Chemical Methods of Rock Analysis*, vol. 1, 3rd ed.; Pergamon: Oxford, 1981.
18. Coey, J. M. D.; Gugat, O.; Mccauley, J.; Fabris, J. D.; *Rev. Fis. Apl. Instrum.* **1992**, *7*, 25.
19. Laboratórium för Argewandte Physik; *NORMOS®90*, DOS version, Universität Duisburg, Duisburg-Germany, 2005.
20. Rodríguez-Carbajal, J.; *Phys. B* **1993**, *192*, 55.
21. Coey, J. M. D. In *Iron in Soils and Clays Minerals*, vol. 217, 1st ed.; Coey, J. M. D.; Stucki, J. W.; Goodman, B. A.; Schwertmann, U., eds.; Reidel Publishing Company: Dublin, 1988, p. 397-466.
22. Russo, U.; Long, G. J. In *Mössbauer Spectroscopy Applied to Inorganic Chemistry*, vol. 2; Long, G. J.; Grandjean, F., eds.; Spring Street: New York, 1987, p. 289-329.
23. Frost, R. B. In *Reviews in Mineralogy*, vol. 25; Lindsley, D., ed.; Chelsea: Michigan, 1991, p. 489-509.
24. Joint Committee on Powder diffraction Standards (JCPDS); *Mineral Powder Diffraction Files Data Book*, 549/.125; Swarthmore International Center Diffraction Data, Swarthmore, Pennsylvania, 1980.
25. Snyder, R. L. In *The Rietveld Method*, 2nd ed.; Young, R. A., ed.; University Press: Oxford, 1995, p. 111-132.
26. Caglioti, G.; Paoletti, A.; Ricci, F. P.; *Nucl. Instrum. Methods Phys. Res., Sect. A* **1958**, *3*, 223.
27. Thompson, P.; Cox, D. E.; Hastings, J. M.; *J. Appl. Crystallogr.* **1987**, *20*, 79.
28. Kniess, C. T.; Lima, J. C.; Prates, P. B.; *The Quantification of Crystalline Phases in Materials: Applications of Rietveld Method*; IntechOpen, 2012.
29. Klug, H. P.; Alexander, L. E.; *X-ray Diffraction Procedures for Polycrystalline and Amorphous Materials*, vol. 2, 1st ed.; John Wiley & Sons: New York, 1974.
30. Wright, J. P.; Attfield, J. P.; Radaelli, P. G.; *Phys. Rev. Lett.* **2002**, *66*, 120.
31. Wright, J. P.; Attfield, J. P.; Radaelli, P. G.; *J. Phys.: Condens. Matter* **2005**, *17*, 7642.
32. Iyengar, S. J.; Joy, M.; Ghosh, C. K.; Dey, S.; Kotnala, R. K.; Ghosh, S.; *RSC Adv.* **2014**, *4*, 64919.
33. Chlan, V.; Żukrowski, J.; Bosak, A.; Kąkol, Z.; Kozłowski, A.; Tarnawski, Z.; Řezníček, R.; Štěpánková, H.; Novák, P.; Biało, I.; Honig, J. M.; *Phys. Rev. B* **2018**, *98*, 125138.

Submitted: January 6, 2020
Published online: April 23, 2020